Northumbria Research Link

Northumbria
University
NEWCASTLE

UniversityLibrary

Wavelet - Artificial Neural Network Receiver for Indoor Optical Wireless Communications

Sujan Rajbhandari, *MIEEE,* Zabih Ghassemlooy, *MIEEE* and Maia Angelova

Abstract— **The multipath induced intersymbol interference (ISI) and fluorescent light interference (FLI) are the two most important system impairments that affect the performance of indoor optical wireless communication (OWC) systems. The presence of either incurs a high optical power penalty (OPP) and hence the interferences should be mitigated with suitable techniques to ensure optimum system performance. The discrete wavelet transform (DWT) and the artificial neural network (ANN) based receiver to mitigate the effect of FLI and ISI has been proposed in the previous study for the one-off keying (OOK) modulation scheme. It offers performance improvement compared to the traditional methods of employing a high pass filter (HPF) and a finite impulse response (FIR) equalizer. In this paper, the investigation of the DWT-ANN based receiver for baseband modulation techniques including OOK, pulse position modulation (PPM) and digital pulse interval modulation (DPIM) are reported. The proposed system is implemented using digital signal processing (DSP) board and results are verified by comparison with simulation data.**

Index Terms—**Optical wireless communication, wavelet transform, artificial neural network**

I. INTRODUCTION

THE increasing popularity of file and video sharing and the possibility of high definition TV broadcast over the internet has already put a huge bandwidth demand on personal communication systems [1, 2]. 4G communication systems promise to support multiple applications and a higher bandwidth per user (>100 Mbps) for indoor and outdoor applications. However, the bandwidth per end-user in existing communication systems is limited to a few Mbps, due to the bottleneck imposed by the use of copper cables or radio frequency (RF) wireless links at the last mile [2]. The solution to the bandwidth congestion and the 'last mile access' bottleneck, is to make the logical move to the optical domain and take advantage of the large, unlicensed optical bandwidth. However, the expansion of fibre-to-the-home in some cases may not be the best solution, considering the cost of deployment. An alternative solution is to adopt the OWC technology that offers security and compatibility with the existing optical fibre backbone [2, 3]. Compared with RF systems, OWC also offers a huge unregulated bandwidth at a single wavelength without resorting to frequency reuse, rapid installation at a low cost and reduced co-channel and adjacent channel interference levels due to the localised radiation foot-print.

Although the combination of intensity modulation/direct detection (IM/DD) that is employed in OWC systems prevents multipath fading, the ambient light interference (ALI) and ISI still constitute major system impairments. The effect of ALI is more severe in indoor applications since the average transmitted optical power level is limited due to the skin and eye-safety considerations. FLI is most severe among the lighting devices used in indoor applications. A number of techniques had been proposed to reduce the effect of FLI including the HPF, angle diversity, optical filtering [4], linear orthogonal polarisers [5] and DWT [6]. Both the digital HPF and the DWT based denoising were considered for OOK in [6] outlining possible performance improvement as well as reduction in system complexity using DWT instead of HPFs. In this study, we take the concept further and apply it to PPM and DPIM schemes, which are widely adopted in OWC systems.

The ISI causes a significant OPP, which increases exponentially with the data rate (or the delay spread). For example, the unequalized OOK modulation scheme incurs a large OPP (> 10 dB) at a normalized delay spread of > 0.50. OPPs would be higher for other modulation schemes with narrower pulse duration such as PPM and DPIM, hence; unequalized reception is not feasible at high data rates for a dispersive channel. Though the maximum likelihood sequence detector (MLSD) is the optimum detector in a dispersive channel, its complexity, delay and high memory requirements are usually too high for practical implementation. In addition, a MLSD is not advocated to the DPIM scheme due to its non-fixed symbol boundary. Therefore, sub-optimal equalization techniques are preferred in practice. Equalizers are classified into linear (without feedback) and decision feedback (DF). In [7, 8], FIR filter based equalization for indoor OWC links employing OOK, PPM and DPIM schemes have been reported. Adaptive equalization is the preferred method in a non-stationary environment. In the traditional approach based on the FIR filters, the filter coefficients are adjusted by transmitting a unique training sequence. The classification capability of the FIR equalizer is limited to a linear decision boundary, which is a non-optimum strategy especially with respect to the time varying channel [9]. The optimum strategy would be to have a hyper-surface boundary for classification. Fundamentally, the equalization problem can be defined as a classification problem and ANNs have been employed as a

classification tool because of its potential to form complex nonlinear decision regions [10]. In [11], ANNs with nonlinear mapping capability have been proposed, showing improved performance.

In this paper, the study of DWT based denoising and ANN based adaptive equalizer for the dispersive indoor OWC channel in the presence of FLI is reported. The proposed receiver is adopted for OOK, PPM and DPIM schemes, though the model can easily be incorporated in any other digital modulation schemes. Further, practical realization of the proposed scheme using a DSP board is also presented. The paper is organised as follows. The performance of OOK, PPM and DPIM indoor OWC systems are discussed in Section II. The concept of DWT based denoising and ANN based equalizers are outlined in Sections III and IV, respectively. The performance of the modulation schemes under test with DWT-ANN based receiver is discussed in Section V followed by the realization of the system in Section VI. Finally, concluding remarks are given in Section VII.

II. INDOOR OWC SYSTEM

Non-return-to-zero (NRZ) OOK format is the most popular and widely utilized digital baseband modulation scheme for OWC systems in which binary '1' is represented by transmitting a pulse of duration T_b (=), where R_b is data rate and binary '0' by an empty slot of duration T_b.

In PPM a symbol of a fixed length consists of slots (or chips) with only one of which is non-zero containing a pulse of constant power. In PPM the information is conveyed by the location of the pulse within the symbol. We denote the PPM symbol by . In order to achieve the same throughput as OOK, PPM slot duration is , where $L = 2^M$ is the symbol length, and M is the bit resolution.

DPIM is an anisochronous pulse modulation scheme, in which each block of M-input data bits $\{d_i, i = 1, 2, ... , M \}$ is mapped to one of L possible symbols { , } of dissimilar length. A symbol is composed of a pulse of one slot duration followed by a sequence of empty slots, the number of which is dependent on the decimal value of the M-bit input data. The average symbol length and the mean slot duration of DPIM are given by:

$$\tag{1}$$

$$\tag{2}$$

Detailed comparisons of different modulation schemes in terms of optical power and bandwidth requirements and reliability are given in [12] and the references therein.

The baseband model of the indoor OWC communication system employing IM/DD in a diffuse channel and in the presence of the FLI interference is shown in Fig. 1, where A is the peak transmitted optical power, m_{fl} is the FLI photocurrent, R is the photodetector responsivity and $n(t)$ is the signal independent shot noise, modelled as additive white Gaussian noise (AWGN). The encoder and decoder must be incorporated at the transmitter and receiver for modulation schemes other than OOK. The transmitter filter has a unit-amplitude rectangular impulse response $p(t)$, with a duration of τ, where τ depends on the modulation scheme ($\tau = T_b$ for OOK; $\tau = T_{s\text{-}PPM}$ for PPM and $\tau = T_{s\text{-}DPIM}$ for DPIM). The peak
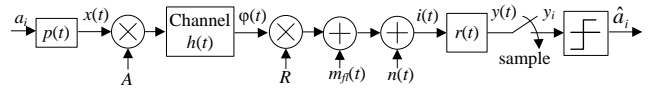

Figure 1: A schematic block diagram of unequalized OOK-NRZ system
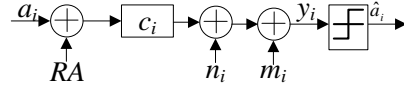

Figure 2: Discrete-time equivalent system for the communication system.

optical power is chosen so that the average transmitted optical power remains the same for all modulation schemes. The receiver consists of a continuous-time filter with an impulse response $r(t)$, which is matched to $p(t)$, followed by a sampler (with a sampling rate $1/\tau$) and a threshold detector. Since the modulation schemes under study are baseband, a similar approach can be adopted to analyse the system performance for all modulation schemes. The channel output of the system given in Fig. 1 can be written as:

$$\tag{3}$$

where $x(t)$ and $i(t)$ are the time dependent channel input and output respectively, denotes convolution.

For simplicity, the system described in Fig. 1 can be modelled using the discrete time equivalent model given in Fig. 2. The discrete-time impulse response of the cascaded system (the transmitter and receiver filters and the channel) is given as:

$$\tag{4}$$

with the normalization and sampling times shifted to maximize the zero-sample .

The sampled FLI and the AWGN n_i are given by:

$$\tag{5}$$

$$\tag{6}$$

A. Performance in an Ideal AWGN Channel

In the absence of noise, the peak output of matched filter (MF) when a 'one' is transmitted is . When a 'zero' is transmitted, the peak output of MF is 0. For a unit-energy MF, the variance of the noise samples at its output is $N_o/2$, where $N_o/2$ is the double-sided power spectral density (PSD) of noise, q is the electron charge and I_B is the average photocurrent generated by the background light.

Therefore, the bit (slot) error probability can be derived as:

$$\tag{7}$$

where is the optimum threshold level, $P(1)$ and $P(0)$ represent the probabilities of one and zero, respectively and $Q(.)$ is the Marcum's Q-function.

Assuming a threshold level set midway between expected one and zero levels (i.e.), (7) reduces to:

$$\tag{8}$$

The average energy per bit E_b is related to the symbol energy as below:

$$\tag{9}$$

$$\tag{10}$$

$$\tag{11}$$

where is the average transmitted optical power.

For PPM with soft decision decoding, rather than considering individual slots, each symbol consisting of L

consecutive slots must be considered as one. Thus, the probability of error for PPM with soft decision decoding is given as [7]:

$$\hspace{6cm} (12)$$

B. Performance in the Presence of FLI (without Filter)

Considering a linear system, P_e in the presence of FLI can be calculated by separately treating the FLI and the modulating signal at the input to the matched filter. Since the interfering signal is periodic, error probability can be estimated by calculating the P_e over the period of interference and averaging it over the same period [13]. By considering every slot over a 20 ms time interval (i.e. one complete cycle of   ) and averaging, the P_e for OOK in the presence of the AWGN and FLI is given by [7, 14]:

$$\hspace{6cm} (13)$$

where N is the total number of bits over a 20 ms interval.

Following the approach taken for OOK, the average slot error rate (SER) for PPM and DPIM with the hard decision scheme can be calculated as [7]:

$$\hspace{6cm} (14)$$

$$\hspace{6cm} (15)$$

The union (upper) bound for the error probability for PPM with the 'soft' decoding scheme is given by [14]:

$$\hspace{6cm} (16)$$

C. Unequalized Performance in a Diffuse Channel

The receiver filter output   in a dispersive channel without noise is given by:

$$\hspace{6cm} (17)$$

where   is the number of channel taps and   is the   bit sequence.

Hence, the average P_e for OOK is approximated by averaging over all possible bits sequence of length ζ as [15]:

$$\hspace{6cm} (18)$$

Unlike OOK,   does not lie in the middle of the '0' and '1' levels for PPM and DPIM due to the unequal probability of the empty slots and pulses. In fact   is a complicated function of M and   . An iterative approach to calculate and approximate P_e is taken in [7]. The iterative approach requires significant computational time, thus is not practical for $\zeta > 20$ [7]. In this work, a constant threshold level   is used, given by:

$$\hspace{6cm} (19)$$

The summation   provides the estimation of the energy of each pulse that has spread to its adjacent pulses due to the dispersive channel. For a LOS link, the summation is zero and hence   . The dispersive channel with a non-zero summation value;   is < 0.5. With the soft decision decoding, a pulse is detected depending upon its relative amplitude within a symbol. Assuming that one occurs in slot q of each symbol, the average symbol error probability for the unequalized PPM with soft decoding is given by [7, 8, 14]:

$$\hspace{6cm} (20)$$

III. DWT BASED DENOISING

The DWT and ANN based receiver for the diffuse indoor channel in the presence of FLI is given in Fig. 3. For simplicity, the wavelet based denoising of FLI is considered in this section and ANN based equalizer in the following section. Unlike the popular wavelet denoising concept in which the effect of Gaussian noise is minimised, the DWT is used here to reduce the low frequency periodic FLI signal whose spectrum can extend from a DC value up to 1 MHz [13, 16]. Hence, to remove the interfering signal from the modulating signal, the received signal is detached into different frequency bands using the DWT decomposition process. The DWT coefficients corresponding to the noise are removed and the signal is reconstructed by the inverse DWT (IDWT) process (see Fig. 7(a)).

The DWT can be realized using successive application of low pass $g(n)$ and high pass $f(n)$ filters and down-sampling by 2. The first level decomposition gives the approximation coefficients y_{1l} and y_{1h} as [17]:

$$\hspace{6cm} (21)$$

$$\hspace{6cm} (22)$$

where l and h refer to the low and high pass filters, respectively. The approximation coefficients can further be decomposed into different DWT coefficient levels with a maximum level of $\log_2 L$, where L is the signal length. For removal of the interfering signal from the received signal, the approximation coefficients, which correspond to the interfering signal, are then made equal to zero so that the reconstructed signal is free from the interfering signal i.e.

$$\hspace{6cm} (23)$$

where γ is the number of the decomposition given by:

$$\hspace{6cm} (24)$$

where   is the floor function and F_c is the desired cut-off frequency.

The signal is subsequently reconstructed using the IDWT process [17]:

$$\hspace{6cm} (25)$$

The detailed description of DWT based denoising and performance of different mother wavelets and comparisons of DWT with HPF is given in the previous publication [6].

IV. AN ANN BASED ADAPTIVE EQUALIZER

Consider a baseband communication system as shown in Fig. 2. In case of a diffuse channel, the discrete received signal is given by:

$$\hspace{6cm} (26)$$

where b_i is noise free channel output, n_i is the AWGN and c_n is the channel tap.

The Lth order equalizer has L-taps with an equally spaced delay of τ for the symbol space equalizer. The channel output can be written in a vector form as:

$$\hspace{6cm} (27)$$
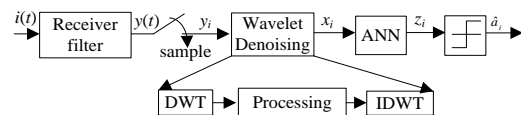

Figure 3: DWT-ANN based receiver in the presence of FLI and ISI.

where T means the transpose operation.

Hence the channel has *L*-dimensional observation space. Depending on the output vector $\mathbf{Y}_i$, the equalizer attempts to classify the receiver vector into one of the two classes: binary zero and binary one. The equalization problem is hence forming a decision boundary that corresponds to the transmitted symbol. Therefore, determining the values of the transmitted symbol with the knowledge of the observation vectors is basically a classification problem [9]. Hence, the generalized nonlinear classification tool such as the ANN can be utilized instead of an equalizer.

The architecture of the ANN based channel equalizer is depicted in Fig. 3. The sample output y_i is passed through tap delay lines (TDLs) prior to being presented to the ANN for channel equalization. The output of the ANN is sliced using   to generate a binary data sequence. In the DF structure, the decision output is fed back to the ANN (see Fig. 7(b)). The length of both the forward and feedback TDLs depend on the channel span, which also depends on the delay spread. Since the ceiling bounce model [18] shows an exponential decay in the channel components, few TDLs are adequate for the optimum performance. The ANN needs to be trained in a supervised manner to adjust its free parameters (weight and bias) to compensate for the ISI. The training is carried out by transmitting a binary sequence for which outputs are known. The details of the ANN training can be found in [6]. The ANN used in this study is the feed-forward back-propagation multilayer perceptron with supervised training and Levenberg–Marquardt algorithms for updating the neural weights.

V. RESULTS AND DISCUSSIONS

In order to make the like-to-like comparisons for different modulation schemes, the normalized average optical power requirement (NOPR) and OPP are defined below:

(a) NOPR: is calculated by normalising the optical power required to achieve a desired SER in an interfering channel with the optical power required to achieve the same SER for the OOK-NRZ system at 1 Mbps in an AWGN channel without interference.

(b) OPP: is calculated by normalising the optical power required to achieve the desired SER in an interfering channel with the optical power required to achieve the same SER in an AWGN channel without interference for the same modulation at the same data rate.

An error probability of 10^{-6} is used as a standard performance metric for evaluation of different modulation techniques [15, 18].

A. Performance in the Presence of FLI and DWT denoising

The FLI model, described in [16], is utilized with an electronic ballast switching frequency of 37.5 kHz. The DWT decomposition level is calculated using (24) with cut-off frequencies of 0.5 MHz and 0.3 MHz for data rates > 10 Mbps and < 10 Mbps, respectively. The 8th member of Daubechies mother wavelet family is used in all simulations as it offers the best performance [6].

The NOPR for the OOK scheme in the presence of FLI and DWT denoising is shown in Fig. 4(a). Also illustrated is the NOPR for the ideal channel without interference. Below a data rate of 10 Mbps, the baseline wander (BLW) effect causes very high OPP and hence the denoising is not effective in reducing the FLI and is not shown in Fig. 4(a). At higher data rates (> 10 Mbps), the DWT can significantly reduce the FLI induced OPP. At 10 Mbps, DWT offers a reduction of ~ 5.5 dB in NOPR compared to the system with no filtering. Higher reduction of ~ 7.4 dB is observed at 40 Mbps. However, this still leaves an OPP of ~ 1.6 dB compared to the same bit rate without interference. The OPP is further reduced at higher data rates with a value of ~ 1.2 dB at 100 Mbps. Note that first order HPF with an optimum cut-off frequency still leaves a OPP of 3 dB at 100 Mbps [7]. The comparative study of HPF and DWT is reported in [6].

The NOPR with DWT denoising for 4, 8 and 16-PPM with hard and soft decision schemes for a data rate of 1-200 Mbps
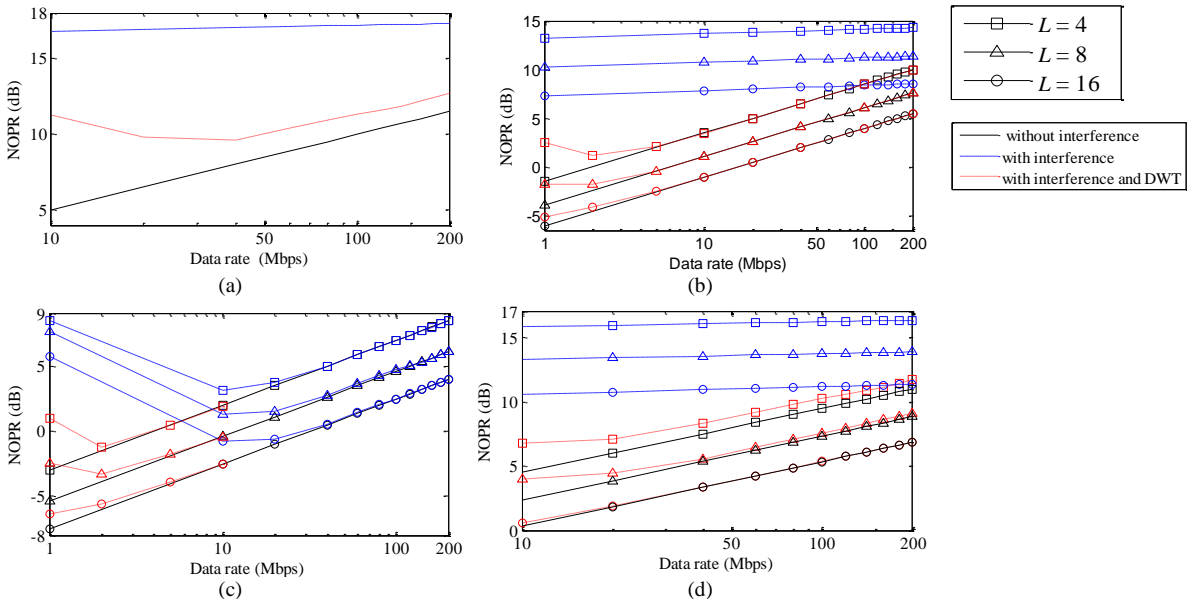

Figure 4: Normalized optical power requirement against data rates with and without DWT denoising in the presence of the FLI (a) OOK, (b) PPM with hard decision decoding, (c) PPM with soft decision decoding and (d) DPIM.

is demonstrated in Figs. 4. For the hard decision decoding, the threshold level is set midway between '1' and '0' levels in the absence of any BLW, given as [7]:

$$\text{(28)}$$

It is clear from Fig. 4(b) that DWT denoising shows a significant reduction in NOPR (~10.7 dB, ~12.1 dB and ~12.4 dB for 4, 8 and 16 PPM, respectively) at a data rate of 1 Mbps for the hard decision decoding. Also, there is a significant reduction in power requirements at 1 Mbps compared to the HPF (HPF requires a NOPR of ~ 7.5 dB, ~ 4 dB and ~ 1.5 dB at 1 Mbps for 4-PPM, 8- PPM and 16-PPM, respectively [7]). Since PPM has no DC component and a low PSD at low frequencies, a higher cut-off frequency can be tolerated without the BLW effect. Hence DWT offers an improvement even at low frequencies for PPM. Above 10 Mbps for 4-PPM and 5 Mbps for the 8 and 16-PPM, the DWT based denoising completely eliminates OPPs due to the FLI. Unlike threshold detection schemes, the soft decision decoding offers immunity to the FLI at data rates > 20 Mbps (Fig. 4(c)). Hence, DWT does not offer any optical gain. However, DWT provides a significant improvement at low data rates. The optical power penalties at 1 Mbps without DWT are ~ 11.5 dB, ~ 13.1 dB and ~13.9 dB for 4, 8 and 16 PPM respectively, which are reduced to ~ 4 dB, ~ 2.9 dB and ~1 dB with DWT denoising.

NOPR for 4, 8 and 16-DPIM at a data rate range of 1 - 200 Mbps with DWT denoising is given in Fig. 4(d). Similar to PPM, α is set midway between one and zero levels in the absence of any filtering and is given as [7]:

$$\text{(29)}$$

Comparing the performance of OOK in Fig. 4(a) and PPM with the hard decision scheme in Fig. 4(b), it can be observed that the performance of DPIM with DWT is between OOK and PPM. Low order DPIM shows performance similar to OOK with constant OPPs compared to the ideal case. However, higher order DPIM shows almost zero OPPs. The phenomenon is due to progressive reduction of the DC and low frequency components with increasing M. Compared to performance without FLI, the power penalties with DWT are ~ 0.7 dB at a data rate > 40 Mbps, which reduces to 0.4 dB for 8-DPIM. The OPPS is reduced to zero by DWT for 16-DPIM at data rates > 20 Mbps.

B. Performance in a Diffuse Link with/without an ANN Equalizer

In this section, it is assumed that the OWC link is dispersive; however FLI is not present. The multipath channel impulse response is given by the ceiling bounce model [18]:

$$\text{(30)}$$

where $u(t)$ is the unit step function, , is the height of the ceiling above the transmitter and receiver and c is the velocity of light. The parameter 'a' is related to root mean square (RMS) delay spread D_{rms} as:

$$\text{(31)}$$

In order to perform like-to-like comparisons of different modulation schemes, a normalized delay spread is used. A two layer multilayer perceptron with log-sigmoid and linear transfer functions is trained in supervised manner with the training length of 1000 bits. The performance of the ANN equalizer is described below.

The NOPR of OOK-NRZ for the ANN based linear and DF equalizers for a range of D_T are illustrated in Fig. 5(a). Also shown is the NOPR for the unequalized case with MF based receiver. The DF scheme offers the least OPP for all range of D_T closely followed by the linear case. Unlike the unequalized system where the irreducible OPP can be observed at $D_T > 0.5$, the equalized cases offer significantly reduced OPP. Both linear and DF schemes demonstrate identical performance for $D_T < 1$ varying only at higher D_T values. Compared to the LOS case ($D_T = 0$), the OPP at $D_T = 2$ is ~ 6 dB for DF equalizer, also OPP is increasing with the delay spread. Two factors have contributed to this OPP: (i) the constant presence of residual ISI particularly when the channel is highly dispersive and (ii) the incorrect decisions being fed back to the equalizer.
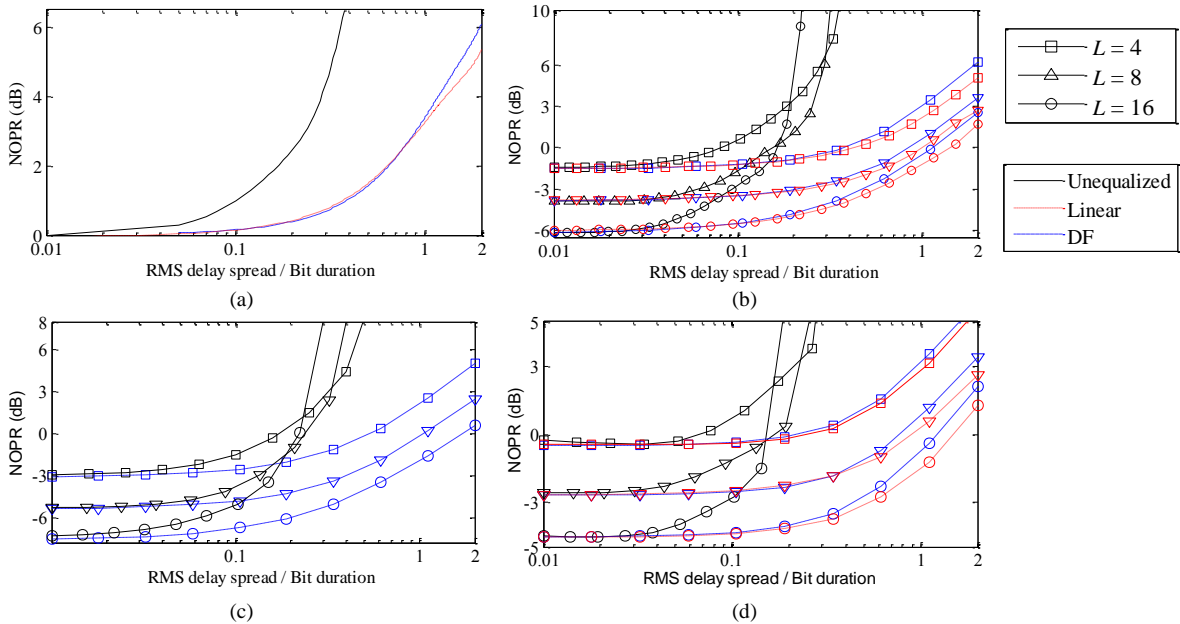

Figure 5: NOPR versus the normalized delay spread for unequalized and ANN equalized schemes (a) OOK, (b) PPM with hard decision decoding, (c) PPM with soft decision decoding and (d) DPIM.

NOPRs for 4, 8 and 16-PPM with an equalizer in a dispersive channel with   of 0-2 is given in Figs. 5 (b) and (c) for hard and soft decision decoding schemes, respectively. The 'soft' decoding provides improved performance compared to 'hard' decoding for all range of D_T and M; though NOPR difference for hard and soft decision decoding schemes decrease as the channel become more dispersive. Similar to the unequalized case, the NOPR for equalized cases also shows an exponential growth. However, the gradients of curves are significantly reduced and do not show the infinite OPPs even at D_T = 2. Note that unlike the unequalized cases, where the higher order PPM system show a sharp rise in the OPP, the equalized system show almost similar profile for all M. The OPP is the highest for 16-PPM with both soft and hard decoding cases due to shortest slot durations. However, equalized 4-PPM and 8-PPM illustrate identical OPPs. Two factors are involved here: (a) the slot duration and (b) the probability of two consecutive pulses. Since 8-PPM has shorter pulse duration, the OPP due to this factor should be higher than that for 4-PPM. On the other hand, due to longer symbol length, the probability of two consecutive pulses is significantly lower for 8-PPM compared to 4-PPM, hence the OPPs related to two consecutive pulses is higher for 4-PPM (avoiding two consecutive pulses can provide significant performance improvement as in case of DPIM [7]). The NOPR of DFE for PPM with hard decision shows a similar trend to OOK. The DFE offers a reduction in OPP compared to the linear equalizer at D_T > 0.2. The simulation confirmed that DFE with soft decoding does not provide any improvement in performance compared to the hard decoding due to the hard decision in the feedback loop and is hence not reported here.

NOPR against the D_T for equalized 4, 8 and 16-DPIM with an ANN based linear equalizer is outlined Fig. 5(d). Also shown is the NOPR of the unequalized system. Similar to other equalized systems, ANN based equalizer shows a significant reduction in NOPR compared to the unequalized cases for D_T > 0.1. Equalization offers ~ 6 dB reduction in NOPR for 4-DPIM compared to the unequalized case at D_T = 0.3. Note that it is not possible to completely eliminate the ISI and hence a nominal OPP occurs for the equalized case if D_T < 0.1 in comparison to the LOS channel. However higher OPP is visible at D_T > 0.1 and the OPP is ~ 6 dB at D_T = 2 for all cases. The DF structure provides improved performance compared to the linear structure for highly dispersive channel and a difference of ~ 0.6 dB is observed at D_T of 1.5.

C. Performance in Diffuse Link in the Presence of FLI

To analyse the effect of the FLI in a diffuse channel, OPP is calculated for different data rates with a fixed value of D_T with a DWT-ANN receiver. The OPP for the OOK system in presence of FLI with D_T of 0, 0.4, 1.2 and 2 at data rates of 20-200 Mbps for the DWT-ANN receiver is depicted in Fig. 6. Since at lower data rates (≤ 10 Mbps), the OWC channel can be practically considered as a LOS, the performance only at higher data rates is reported here. The OPP increases as the channel becomes more dispersive; channels with D_T = 2 showing the largest OPP whereas a LOS (D_T = 0) link show

the least OPP. For a fixed value of D_T, the OPP decreases with increasing data rates as OPP due to FLI decreasing with the increasing data rates. For the channel with D_T of 2, the OPP reduces from ~ 9.6 dB at a data rate of 20 Mbps to 6.8 dB at a data rate > 100 Mbps. The OPP curves are almost parallel to the LOS (D_T = 0) curve, which indicates that the overall OPP in the presence of FLI and ISI is summation of individual OPPs. With this observation, it is safe to say that FLI effect would be negligible in PPM and DPIM schemes at higher data rates due to effectiveness of DWT to mitigate FLI.

VI. System Realization

The implementation of the DWT-ANN based receiver in a commercially available DSP board (TI TMS320C6713) is reported in this section. The Simulink models for implementation of DWT based denoising and ANN based equalizer are given in Figs. 7 (a) and (b), respectively. Note that the equalizer can be modified to make it linear or DF as necessary. The system is implemented in the DSP module by converting the Simulink model to the assembly code. In order to verify the practical results, the real-time data exchange (RTDX) link is used to transfer data between the DSP board and the computer. For the simplicity of design, the optimum weight and bias for the ANN is calculated using computer simulation and then exported to the DSP board.

In order to verify the practical results, an error signal e_r is calculated by subtracting MATLAB output with DSP output. The square of error signal for sample values for the DWT based denoising scheme is demonstrated in Fig. 8. It can be observed that except for the initial phases, the error signal e_r is significantly low, in the range of 10^{-6}. Since the outputs are sliced using a threshold value of zero, the low value of e_r does not significantly affect the error probability of the system. This provides evidence that the DWT based denoising can be successfully implemented in the DSP having capability of floating point operations. In order to verify the successful implementation of ANN based equalizer in DSP board, the bit error rate (BER) is calculated from the DSP board output and compared with the simulation results. Measured and calculated (using the computer simulation) BER for the ANN equalizer for a range of signal-to-noise (SNR) values is given in Table I. It can be seen that the two results are strikingly similar indicating the successful implementation of the ANN in the DSP board.
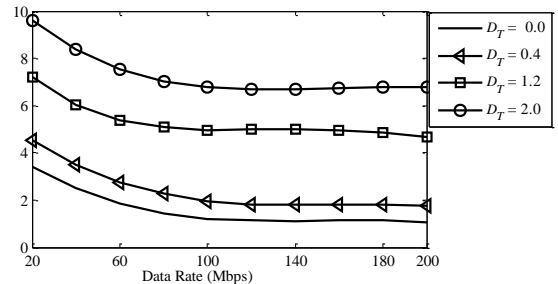

Figure 6: OPP versus the data rates for the DWT-ANN based receiver the OOK scheme with the D_T of 0, 0.4, 1.2 and 2 in presence of the FLI.
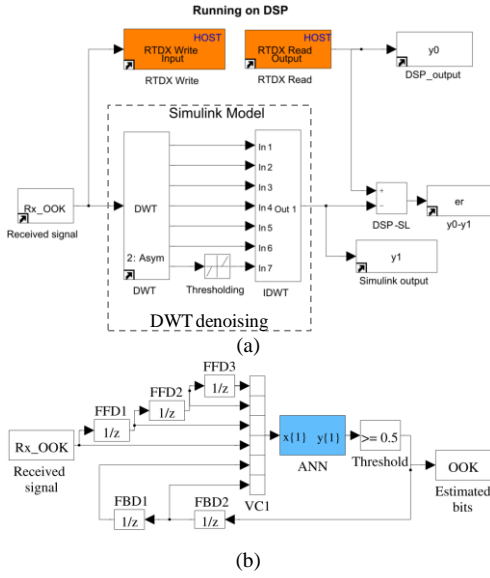
(a)

(b)

Figure 7: Simulink model of a) DSP implementation of the DWT based denoising and b) ANN based DFE structure. FFD: feedforward delay; FBD: feedback delay.
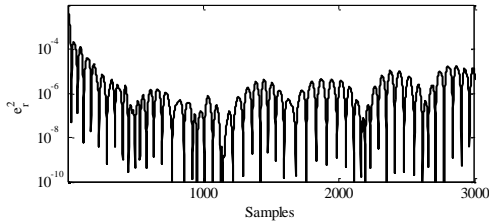

Figure 8: Square of error signal e_r between the DSP output and Matlab outputs for DWT based denoising scheme against number of samples.

TABLE I
THE BER CALCULATED USING THE SIMULINK MODEL AND DSP IMPLEMENTATION

SNR (dB)	BER(DSP)	BER(Simulation)
10	0.197	0.197
16	0.0669	0.052
18	0.023	0.023
20	0.0012	0.0012

VII. CONCLUSION

The paper summarised the effectiveness of DWT and ANN to reduce the adverse effects of FLI and multipath induced ISI, in indoor OWC systems. The baseband modulation techniques OOK, PPM and DPIM were selected for the comparative studies. The studies showed that PPM with soft decision decoding offers the highest resilience to FLI and ISI and outperforms systems with threshold detection schemes. Due to the high spectral power density at low frequencies, OOK scheme show higher OPP and BLW effect in the presence of DWT. At high data rate, DWT offers significant improvement and an OPP of ~ 1.2 dB is observed. However, the DWT completely eliminates the effect of FLI for PPM. Higher order of DPIM show similar characteristic as PPM, however characteristic at lower order is similar to OOK. The ANN is effective in reducing the effect of ISI in a multipath channel and unlike unequalized cases; the OPPs of the equalized

system were significantly lower even at the normalized delay spread of 2. The proposed DWT-ANN based receiver was successfully realized using a commercially available DSP board and practical results are verified by comparing them with the simulation data.

REFERENCES

[1] W. Ke, A. Nirmalathas, C. Lim, and E. Skafidas, "4×12.5 Gb/s WDM Optical Wireless Communication System for Indoor Applications," *Lightwave Technology, Journal of,* vol. 29, pp. 1988-1996.

[2] D. O'Brien, G. Parry, and P. Stavrinou, "Optical hotspots speed up wireless communication," *Nature Photonics,* vol. 1, pp. 245-247, 2007.

[3] R. J. Green, H. Joshi, M. D. Higgins, and M. S. Leeson, "Recent developments in indoor optical wireless systems," *IET Communications,* vol. 2, pp. 3-10, 2008.

[4] A. J. C. Moreira, R. T. Valadas, and A. M. Duarte, "Reducing the effects of artificial light interference in wireless infrared transmission systems," in *Proceedings of IEE Colloquium on Optical Free Space Communication Links*, London, U.K, 1996, pp. 5/1-5/10.

[5] S. Lee, "Reducing the effects of ambient noise light in an indoor optical wireless system using polarizers," *Microwave and Optical Technology Letters,* vol. 40, pp. 228-230, 2004.

[6] S. Rajbhandari, Z. Ghassemlooy, and M. Angelova, "Effective denoising and adaptive equalization of indoor optical wireless channel with artificial light using the discrete wavelet transform and artificial neural network," *IEEE/OSA Journal of Lightwave Technology,* vol. 27, pp. 4493-4500, 2009.

[7] A. R. Hayes, "Digital pulse interval modulation for indoor optical wireless communication systems," PhD thesis, Sheffield Hallam University, UK, 2002.

[8] D. C. Lee and J. M. Kahn, "Coding and equalization for PPM on wireless infrared channels," *IEEE Transaction on Communication,* vol. 47, pp. 255-260, 1999.

[9] L. Hanzo, C. H. Wong, and M. S. Yee, "Neural networked based equalization," in *Adaptive wireless transceivers*: Wiley-IEEE Press, 2002, pp. 299-383.

[10] C. Ching-Haur, S. Sammy, and W. Che-Ho, "A polynomial-perceptron based decision feedback equalizer with a robust learning algorithm," *Signal Processing,* vol. 47, pp. 145 - 158 1995.

[11] A. Hussain, J. J. Soraghan, and T. S. Durrani, "A new adaptive functional-link neural-network-based DFE for overcoming co-channel interference," *IEEE Transactions on Communications,* vol. 45, pp. 1358-1362, 1997.

[12] Z. Ghassemlooy, and *et. al.* "A synopsis of modulation techniques for wireless infrared communication," *ICTON Mediterranean Winter Conference (ICTON-MW),* pp. 1-6, 2007.

[13] A. J. C. Moreira, R. T. Valadas, and A. M. d. O. Duarte, "Performance of infrared transmission systems under ambient light interference," *IEE Proceedings -Optoelectronics,* vol. 143, pp. 339-346, 1996.

[14] R. Narasimhan, M. D. Audeh, and J. M. Kahn, "Effect of electronic-ballast fluorescent lighting on wireless infrared links," *IEE Proceedings - Optoelectronics,* vol. 143, pp. 347-354, 1996.

[15] J. R. Barry, J. M. Kahn, W. J. Krause, E. A. Lee, and D. G. Messerschmitt, "Simulation of multipath impulse response for indoor wireless optical channels," *IEEE Journal on Selected Areas in Communications,* vol. 11, pp. 367 - 379, 1993.

[16] A. J. C. Moreira, R. T. Valadas, and A. M. d. O. Duarte, "Optical interference produced by artificial light," *Wireless Networks,* vol. 3, pp. 131-140, 1997.

[17] C. S. Burrus, R. A. Gopinath, and H. Guo, *Introduction to wavelets and wavelet transforms: A primer* New Jersey: Prentice Hall, 1998.

[18] J. B. Carruthers and J. M. Kahn, "Modeling of nondirected wireless Infrared channels," *IEEE Transaction on Communication,* vol. 45, pp. 1260-1268, 1997.